Meat Science 216 (2024) 109580

Contents lists available at ScienceDirect

Meat Science

journal homepage: www.elsevier.com/locate/meatsci

S-nitrosoproteomics profiling elucidates the regulatory mechanism of S-nitrosylation on beef quality

Qin Hou [a,b], Tianyi Gao [a], Rui Liu [c], Chao Ma [b], Wangang Zhang [b,*]

[a] School of Tourism and Cuisine, Yangzhou University, Industrial Engineering Center for Huaiyang Cuisine of Jiangsu Province, Yangzhou, Jiangsu 225127, China
[b] Key Laboratory of Meat Processing and Quality Control, Ministry of Education China, Jiangsu Collaborative Innovation Center of Meat Production and Processing, Quality and Safety Control, College of Food Science and Technology, Nanjing Agricultural University, Nanjing, Jiangsu 210095, China
[c] College of Food Science and Engineering, Yangzhou University, Yangzhou, Jiangsu 225127, China

ARTICLE INFO

Keywords:
S-nitrosylation
Differential S-nitrosylated proteins
Nitrosoproteomics
Metabolic pathways
Beef quality

ABSTRACT

This study aimed to quantitively profile the S-nitrosylation in beef *semimembranosus* (SM) with different treatments (nitric oxide donor or nitric oxide synthase inhibitor) by applying iodoTMT-based nitrosoproteomics. Results showed that 2096 S-nitrosylated cysteine sites in 368 proteins were detected in beef SM. Besides, differential SNO-modified proteins were screened, some of which were involved in crucial biochemical pathways, including calcium-releasing-related proteins, energy metabolic enzymes, myofibrils, and cytoskeletal proteins. GO analysis indicated that differential proteins were localized in a wide range of cellular compartments, such as cytoplasm, organelle, and mitochondrion, providing a prerequisite for S-nitrosylation exerting broad roles in post-mortem muscles. Furthermore, KEGG analysis validated that these proteins participated in the regulation of diverse post-mortem metabolic processes, especially glycolysis. To conclude, changes of S-nitrosylation levels in post-mortem muscles could impact the structure and function of crucial muscle proteins, which lead to different levels of muscle metabolism and ultimately affect beef quality.

1. Introduction

Nitric oxide (NO) emerges as a potent biological modulator, which performs crucial functions in muscle contraction, respiration, and glucose uptake (Hess et al., 2005). Nitric oxide synthase (NOS)-dependent pathway is recognized as the principal source of endogenous NO in skeletal muscle (Stamler et al., 2008). Studies have documented the activation of NOS in post-mortem trout, chicken, pork, and beef (Brannan & Decker, 2002; Hou et al., 2019). Most notably, NOS retained its activity during 14 days of beef aging (Hou et al., 2019), which could provide the possibility for the sustained production of NO and its involvement in post-mortem beef metabolism. Currently, studies regarding the contribution of NO to meat quality have been conducted by manipulating NO levels in post-mortem muscles, whereas the findings remain contradictory (Cottrell et al., 2008; Hou et al., 2020; Zhang et al., 2019). It is proposed by Liu et al. (2018) that different levels of NO generated in muscle cells play roles in the regulation of biochemical reactions during post-mortem aging, which causes differences in meat quality. However, the specific mechanism of NO in regulating meat quality is still not elucidated.

Generally, NO exerts its functions through three signaling pathways, namely the cGMP pathway, cytochrome oxidase pathway, and protein S-nitrosylation (Horenberg et al., 2019). The covalent combination of NO with cysteine thiols is termed protein S-nitrosylation. It is commonly asserted that S-nitrosylation can critically modulate diverse physiological processes through altering protein structure, subcellular localization, or protein-protein interaction (Hess et al., 2005). Interestingly, recent studies have revealed the modification of S-nitrosylation on specific proteins for regulating muscle cellular functions, including μ-calpain and caspase-3 (Hou et al., 2022; Liu et al., 2016). It implies that NO-induced S-nitrosylation might influence meat quality by altering the structure and function of crucial muscle proteins. However, a limited number of S-nitrosylated targets regarding post-mortem muscle were identified specifically, restricting the deeper profiling of S-nitrosylation. Therefore, a large-scale identification of S-nitrosylation is urgently required.

To date, much effort has been made towards the specific identification of S-nitrosylated proteins (SNPs) and cysteine sites (SNCs). The biotin switch technique (BST) was first proposed by Jaffrey et al. (2001) that free thiols were blocked with MMTS followed by selective reduction

* Corresponding author at: College of Food Science and Technology, Nanjing Agricultural University, Nanjing, Jiangsu 210095, China.
E-mail address: wangang.zhang@yahoo.com (W. Zhang).

https://doi.org/10.1016/j.meatsci.2024.109580
Received 16 April 2024; Received in revised form 19 June 2024; Accepted 21 June 2024
Available online 24 June 2024

by ascorbate to reform the thiols, which were then reacted with the biotin-HPDP to achieve selective enrichment. However, due to the ability of MMTS to compete with biotin-HPDP for thiol groups, limited SNPs were identified using BST. As a result, the BST assay was modified to enhance the efficacy and precision of SNP identification (Figueired et al., 2015; Forrester et al., 2009). Recently, BST coupled with tandem mass tags (TMT) was adopted to quantify SNO modifications in post-mortem pork (Liu et al., 2019). Besides, iodoTMT-based proteomics has become the major strategy for labeling and enriching S-nitrosopeptides (Qiu et al., 2019; Qu et al., 2014). We recently compared SNO-modified proteins and sites between intermediate pHu and high pHu beef using the iodoTMT proteomic technique, indicating the potential impact of S-nitrosylation on muscle pH (Zhu et al., 2021).

To further explore the mechanism of NO-induced S-nitrosylation on beef quality, the first comprehensive analysis of S-nitrosylation in post-mortem beef SM was performed in this study by exogenous regulation of S-nitrosylation level. Quantitative S-nitrosoproteomic was utilized in this study to determine differential SNPs and SNCS in beef SM muscles treated with NO donor or NOS inhibitor. Besides, bioinformatics analysis was conducted to explore the crucial biochemical pathways in which differential proteins were involved in early post-mortem conversion of muscle into meat. This study could give more insights into the comprehensive roles of NO-induced S-nitrosylation in post-mortem muscles, which could provide valuable information for us to better elucidate the underlying mechanism of S-nitrosylation in modulating the development of beef quality.

2. Materials and methods

2.1. Animal and muscle samples

Five Luxi hybrid cattle (Simental × Luxi cattle, 20 months of age, with the weight of 480 ± 20 kg, under identical feeding management conditions) were selected from a commercial farm (Guangfu Animal Husbandry Co., Ltd., Shandong, Yangxin). Following that, slaughtering was conducted based on GB/T 19477–2018 and beef *semimembranosus* muscles (SM, only right side) were taken immediately after slaughter. Based on our pre-experiment results, beef SM muscles exhibited higher NOS activity and S-nitrosylation level, thus SM muscles were selected for further S-nitrosoproteomics analysis in the current study. Collected SM muscles were subjected to pH values and color measurement and assessed as normal meat (Hou et al., 2020). Besides, each SM muscle was sub-sectioned into 3 chunks, which were randomly numbered 1–3 for different treatments. The muscles labeled with the same number were allocated to the same treatment group. This suggests that five samples for each treatment group were collected from five carcasses ($n = 5$). Then each chunk was sliced to three samples of muscle 5 cm × 5 cm × 1.5 cm and randomly immersed in the following solution at a ratio of 1:1 (*w/v*): control group (100 mM NaCl, CON), NO donor (200 μM S-nitrosoglutathione, GSNO), and NOS inhibitor (100 mM NG-monomethyl-L-arginine, L-NAME). Specific muscle cutting and preparation are shown in Supplementary Fig. 1. The concentration of NO donor and NOS inhibitor was chosen according to Zhang et al. (2018). After incubation for 24 h, the surface of muscles was patted dry using filter paper. Then obtained samples were divided into two portions, among which one portion was used to determine beef pH, color, and shear force while the remaining portion was chopped and placed in the cryopreservation tubes followed by quickly frozen in liquid nitrogen and then stored at −80 °C for later use.

2.2. S-nitrosothiol levels

The S-nitrosothiol (SNO) changes in SM muscles were determined using the Saville assay (Su et al., 2013). One gram of muscle sample was added into 5 mL of extraction solution (0.05 M NH_4HCO_3, 0.05 M NaCl) for homogenization at 8000 rpm under ice bath conditions followed by centrifugation at 10,000 ×*g* for 10 min. The protein concentration of the supernatant was assayed and adjusted to 1 mg/mL with 0.25 M HEPES and 1 mM EDTA. Subsequently, 50 μL protein extracts were taken and reacted with 50 μL solution A (1% sulfanilamide, 0.5 M HCl) or solution B (0.2% $HgCl_2$ in solution A) for 5 min. After that, 100 μL solution C (0.02% N-(1-naphthyl) ethylenediamine dihydrochloride, 0.5 M HCl) was added. Immediately after incubation for 5 min, the absorbances of the samples were measured at 540 nm. The standard solution (200 μM GSNO) was used to prepare the standard curve, and the absorbance values of samples were used to calculate the content of SNO according to the standard curve.

2.3. Determination of beef quality

The pH of beef SM muscle was evaluated by referring to the procedures of Wang et al. (2019) with slight modifications. A portable pH meter (HI9025, Hanna, Italy) was utilized to measure the pH of SM muscles at 45 min and 24 h post-mortem. Before the measurement, it was calibrated with standard solutions of pH 4.0 and 7.0, and then the pH of beef samples was measured at five locations and the average value was calculated. Color measurement was performed as described by Cottrell et al. (2008). SM muscles were cut horizontally and then allowed to bloom for 20 min. After this time, color measurement was performed using the colorimeter (CR-400, Minolta, Japan) with L^*, a^*, b^* system, light source D65, C8mm, and 2° observer. The chromameter was calibrated on a white calibration plate (Y = 87.9, x = 0.3158, y = 0.3324) prior to measurement. The average of three measurements was taken across the same cross section of muscle avoiding areas of connective tissue or intramuscular fat. Besides, C^*, h^* were calculated based on the following formulas:

$$C^* = \left[(a^*)^2 + (b^*)^2\right]^{1/2}.$$

$$h^* = arctan(b^*/a^*).$$

In addition, the shear force of SM muscle was determined as described by Zhu et al. (2021). Beef samples (5 cm × 5 cm × 1 cm) were put into cooking bags and heated in a water bath until the center of beef samples reached 70 °C. Then samples were cooled down to 25 °C with running water. Following that, the cooked beef was cut along the direction of the muscle fiber to obtain six meat strips of 4 cm × 1 cm × 1 cm. The shear force of meat strips were determined using a tenderness instrument (XL1155, Tenovo, China). The shear velocity was 5 mm/s and results were expressed as newton (N).

2.4. S-nitrosylation identification by iodoTMT S-nitroproteomics

The iodoTMT S-nitroproteomics were utilized to quantitively identify S-nitrosylated proteins and sites of beef SM muscles and the schematic is presented in Fig. 1. First, minced beef samples were added with extracting solution (0.1 M Tris-HCl, 4% SDS) and then sonicated under an ice bath for 2 min. After centrifugation at 10,000 ×*g* and 4 °C, 1 mg of protein was taken and reacted with 0.1 M NEM overnight to block free thiol groups of cysteines. After removing residual NEM by acetone precipitation, the protein precipitate was redissolved in 1 mL PBS containing 6 M urea and 2% SDS. Subsequently, 20 mM sodium ascorbate, 5 mM EDTA, 4 mM Biotin-HPDP, and protease inhibitor was added and mixed gently for incubation at 25 °C for 1.5 h. Afterwards, the proteins were concentrated and then resuspended in 8 M UA solution. The trypsin digestion of the biotin-labeled proteins was followed by C18 column enrichment. An equal amount of peptides was taken and mixed with 100 μL high-capacity neutravidin beads for 1 h. The buffer (0.5 M NaCl, 0.2% SDS) and PBS were used to wash the beads five times and four times, respectively. After that, iodo-TMT with reporter ions from 126 to 130 were added to label the peptides. Excess labeling reagent was

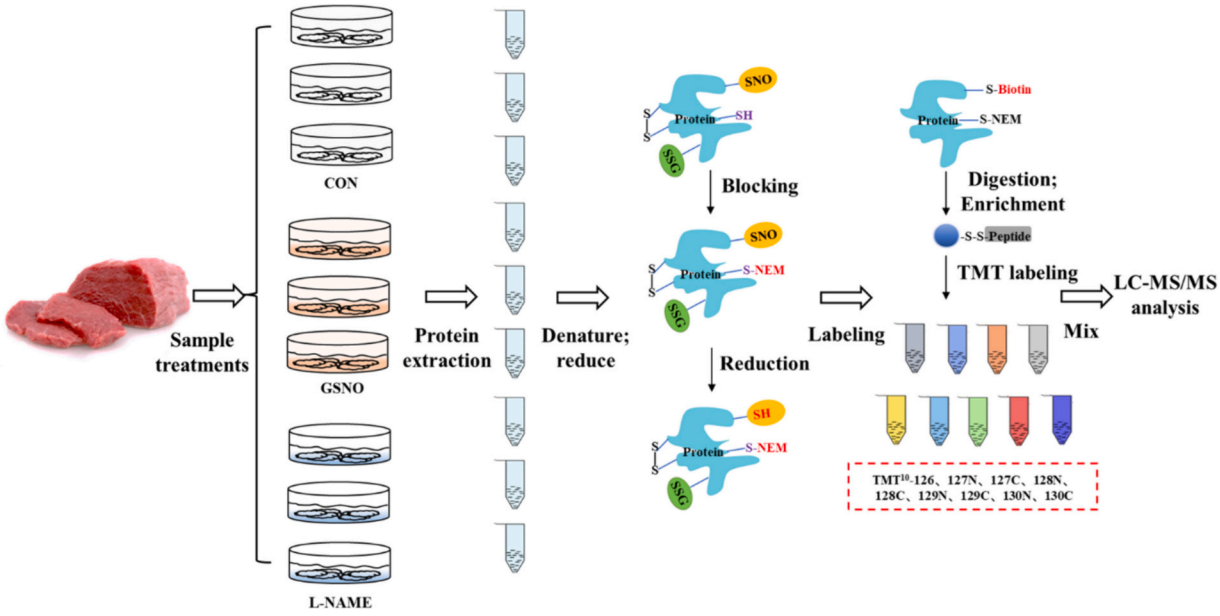

Fig. 1. Schematic of iodoTMT quantitative proteomics to detect S-nitrosylated proteins and sites in postmortem beef *semimembranosus* muscles with three treatments. CON: the control group, GSNO: NO donor group, L-NAME: NOS inhibitor group.

washed three times using PBS. Elution buffer (0.05 M NH_4HCO_3, pH 8.2) and 5 mM TCEP were used to elute the peptides. The elution was repeated once, and 20 mM IAA was added for reaction in the dark for 1 h. After the reaction, the peptides were desalted after drying and then subjected to vacuum concentration. Then peptides were dissolved in 10 μL of 0.1% formic acid for subsequent analysis.

The enriched peptides were chromatographically separated using the Easy nLC 1200 chromatographic system (Thermo, RD, USA). Buffer was composed of solution A (0.1% formic acid solution) and solution B (0.1% formic acid-acetonitrile solution). Solution A (95%) was used to equilibrate the column. Samples were injected into the Trap Column and passed through the chromatographic analysis column for gradient separation with a 300 nL/min flow rate. The separated peptides were subjected to mass spectrometry (MS) analysis as follows: analysis time (240 min), detection mode (positive ion), precursor ion scan range (350-1800 *m/z*), primary MS resolution (60, 000 @m/z 200), AGC target (3e6), primary maximum IT (50 ms). Acquisition of an MS2 scan with 15 highest-intensity precursor ions was triggered after each full scan. Analysis was conducted according to the following parameters: MS2 resolution (45, 000 @m/z 200), AGC target (1e5), secondary Maximum IT (50 ms), MS2 Activation Type (HCD), Isolation window (1.6 Th), and Normalized collision energy (32).

2.5. Database search

Final LC-MS/MS raw data analysis was performed using Maxquant software (version 1.6.1.0). The parameters for the Maxquant database search were set as follows: Type (reporter ion MS2), Isobaric labels (TMT 6 plex), Enzyme (trypsin), Main search Peptide Tolerance (10 ppm), MS/MS Tolerance (0.02 Da), Fixed modifications (TMT6plex (K)), Variable modifications: Oxidation (M), Acetyl (Protein N-term), TMT6plex (Peptide N-term), NEM (C), Deamidation(N/Q), Carbamidomethyl (C), Database (Uniprot-*Bos taurus* (Bovine) _46754_20210203.fasta), Database pattern (Target-Reverse), PSM FDR $\leq$ 0.01, and Protein FDR $\leq$ 0.01.

2.6. Bioinformatics analysis

All identified protein sequences were annotated to the Gene Ontology (GO) identifiers using the InterProScan (version 5.52–86.0). The 'top GO' package was used to complete GO functional classification and statistics analysis. Besides, KOBAS (version 3.0.3) was used to obtain the Kyoto Encyclopedia of Genes and Genomes (KEGG) terms associated with the differential proteins. To perform protein-protein interaction (PPI) network, a String Network was generated using the Cytoscape (http://www.omicsbean.com) based on 4 levels of functional analysis: fold-change of protein expression, protein-protein interactions, KEGG pathway enrichment, and biological process enrichment. Circle nodes refer to genes/proteins. A default confidence cutoff of 400 was used. The rectangles refer to KEGG pathways, colored with gradient colors from yellow (smaller *P* value) to blue (larger *P* value). Genes/proteins are colored in red (up-regulation) and green (down-regulation). Interactions with larger confident scores are indicated with solid lines between genes/proteins, or otherwise shown as dashed lines.

2.7. Statistical analysis

The experimental data were analyzed using SPSS 25.0 software (IBM Corporation, USA). One-way analysis of variance (ANOVA) combined with Tukey's multiple range test was used to examine the differences of pH, color, shear force, and SNO levels among samples from different treatments ($P < 0.05$, $n = 5$). Besides, three treatments (CON, GSNO, and L-NAME) were considered as the fixed term while SM muscle was included as a random term, which referred to the reports of Biffin et al. (2020) and Liu et al. (2021). The results were expressed as mean ± standard error (SE). Hierarchical clustering heatmap and volcano plot were constructed based on S-nitrosylated protein abundance of beef SM samples using R language package at the OmicsBean platform (http://www.omicsbean.cn/). The false discovery rate (FDR) of peptide spectral matches and protein was set to below 0.01. The fold change >1.2 and $P < 0.05$ were utilized as cutoff values to screen the differential specific SNO-sites modification among different groups referring to Zhu et al. (2021).

3. Result and discussion

3.1. Exogenous regulation of S-nitrosylation

Employing NO donor or NOS inhibitor is recognized as the main approach to explore the regulatory effects of S-nitrosylation on meat

quality (Liu et al., 2018). As a primary endogenous NO donor, GSNO can release NO through light or metal ion catalysis under room temperature conditions (Miller & Megson, 2007). Besides, GSNO can serve as a carrier for the transportation of NO groups to balance the level of SNOs in the body through denitrosylation and transnitrosylation reactions (Wang et al., 2002). Accordingly, GSNO was widely chosen to facilitate S-nitrosylation. Furthermore, NOS can catalyze the conversion of arginine to NO and citrulline. A host of small molecules could block the activity of NOS and then restrain the formation of NO (Alderton et al., 2001). Among these, L-arginine analogs were the most widely used NOS inhibitors, which can competitively bind to the catalytic sites of NOS with arginine. The common L-arginine analogs include L-NMMA, L-NNA, and L-NAME. Herein, GSNO and L-NAME were employed in the manipulation of S-nitrosylation level in beef SM muscle.

The S-nitrosylation level of post-mortem beef can be assessed by measuring the content of SNO (Su et al., 2013). As can be seen from Fig. 2, the SNO level of the GSNO group was noticeably higher than the control ($P < 0.05$), whereas it significantly dropped in the L-NAME group. This suggests that S-nitrosylation levels of beef muscles were elevated by GSNO while suppressed by L-NAME. The increased S-nitrosylation level in the GSNO group could be explained by the ability of GSNO to endogenously produce NO and subsequently induce S-nitrosylation. In addition, L-NAME could exert an inhibitory effect on NOS activity and repress the generation of NO, hence impeding the NO-induced S-nitrosylation. This was evidenced by Zhang et al. (2018) that S-nitrosylation levels of beef samples showed a considerable increase when treated with 200 μM and 400 μM GSNO, but decreased in 100 mM and 150 mM L-NAME groups. It is derived that manipulation of S-nitrosylation levels in beef SM muscle was successfully carried out through exogenous incubation with NO donor or NOS inhibitor in the current study.

3.2. Beef quality

The changes in beef quality after treatments with NO donor (GSNO) or NOS inhibitor (L-NAME) are shown in Table 1. The pH values of SM muscles were not affected by NO donor or NOS inhibitor incubation at 24 h post-mortem when compared to the control ($P > 0.05$), whereas the

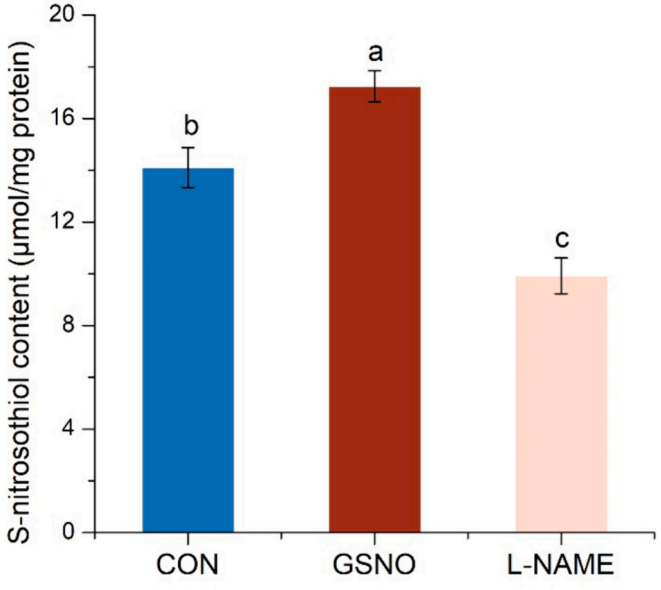

Fig. 2. Comparison of S-nitrosothiol content at 24 h postmortem among different treatments. Data are expressed as mean ± standard error. a-c: different letters indicate significant differences ($P < 0.05$, n = 5). CON: the control group, GSNO: NO donor group, L-NAME: NOS inhibitor group.

Table 1
The pH, color, and shear force of beef *semimembranosus* muscles among different treatments.

Beef quality	CON	GSNO	L-NAME
pH_{45min}	6.20 ± 0.04^{a}	6.18 ± 0.06^{a}	6.15 ± 0.03^{a}
pH_{24h}	5.48 ± 0.03^{ab}	5.53 ± 0.04^{a}	5.37 ± 0.04^{b}
L^*	40.4 ± 1.24^{b}	40.6 ± 1.25^{b}	44.0 ± 1.01^{a}
a^*	11.0 ± 0.10^{b}	12.1 ± 0.35^{a}	10.5 ± 0.51^{b}
b^*	4.5 ± 0.12^{a}	4.6 ± 0.30^{a}	4.5 ± 0.26^{a}
C^*	12.0 ± 0.14^{b}	13.0 ± 0.36^{a}	11.4 ± 0.46^{b}
h^*	22.1 ± 0.58^{a}	20.8 ± 1.31^{a}	23.4 ± 1.60^{a}
Shear force (N)	61.6 ± 1.05^{b}	64.8 ± 0.97^{a}	57.8 ± 1.09^{c}

Note: Data are expressed as means ± standard error (n = 5). Means with different superscripts within the rows are significantly different ($P < 0.05$). CON: the control group, GSNO: NO donor group, L-NAME: NOS inhibitor group.

pH value of the NOS inhibitor group was significantly lower than the NO donor group ($P < 0.05$). Similarly, Cottrell et al. (2008) and Zhang et al. (2013) found that NO donor and NOS inhibitor treatments did not show significant effects on the pH values of beef SM and chicken muscles. Conversely, a recent study indicated that the pH value of pork *longissimus lumborum* in the NOS inhibitor group was remarkably lower than the control group and the variations in glycolysis induced by NO in post-mortem pork may account for pH differences (Zhang et al., 2019). The discrepancy might be attributed to different regulations of NO levels among various species and muscle fibers. In addition, L-NAME-treated SM muscle showed higher L^* values compared with the control and GSNO groups ($P < 0.05$). In terms of a^* value, GSNO treatment significantly increased a^* value of SM muscle ($P < 0.05$), probably due to the high levels of NO, which could react with myoglobin to produce nitrosomyoglobin (Moller & Skibsted, 2002). However, no significant change was detected in the b^* value among the three treatments ($P > 0.05$). It was indicated that compared to the control group, C^* value of beef SM muscle was increased by GSNO treatment while decreased by L-NAME treatment ($P < 0.05$). However, h^* value did not reveal any significant differences among three treatment groups ($P > 0.05$). This result was in accordance with the report of Zhu et al. (2021) that higher S-nitrosylation degree was detected in high pHu beef compared to intermediate pHu beef, however, no significant difference of h^* value was found in high and intermediate pHu beef, indicating that protein S-nitrosylation could not cause impact on the h^* value of SM muscle. As noted above, S-nitrosylation was implicated in regulating beef color development. Most notably, the shear force value of SM muscle was markedly enhanced in the GSNO group while decreased in the L-NAME group ($P < 0.05$), indicating that NO-mediated S-nitrosylation prominently affected beef tenderness. Regulation of μ-calpain activation and myofibril degradation by S-nitrosylation could account for the changes in beef tenderness (Hou et al., 2020). From the results above, it was conceivable that S-nitrosylation can exert regulatory impacts on beef quality, especially on tenderness.

3.3. Quantitative S-nitroproteomics analysis in post-mortem beef

To explore the regulatory pathways of S-nitrosylation on beef quality, iodoTMT-based S-nitroproteomics were performed in this paper. It was mainly composed of four steps, namely the blocking of free cysteines by NEM, the reduction of S-NO bounds by ascorbate, the labeling of iodoTMT, and the identification of S-nitrosylation by LC-MS/MS (Fig. 1). It has been proven that the TMT-labeled approach could enormously enhance the ability to identify S-nitrosylated peptides, with a 40%–85% increase in enrichment efficiency compared to the BST assay (Zhu et al., 2021). According to Fig. 3(a), a host of 2336 modified peptides was detected, revealing the rich data on the S-nitrosoproteome of beef SM muscle. Specifically, 2096 SNO-modified cysteine sites (SNCs) belonging to 368 proteins (SNPs) were identified, suggesting that a significant quantity of proteins was susceptible to S-nitrosylation

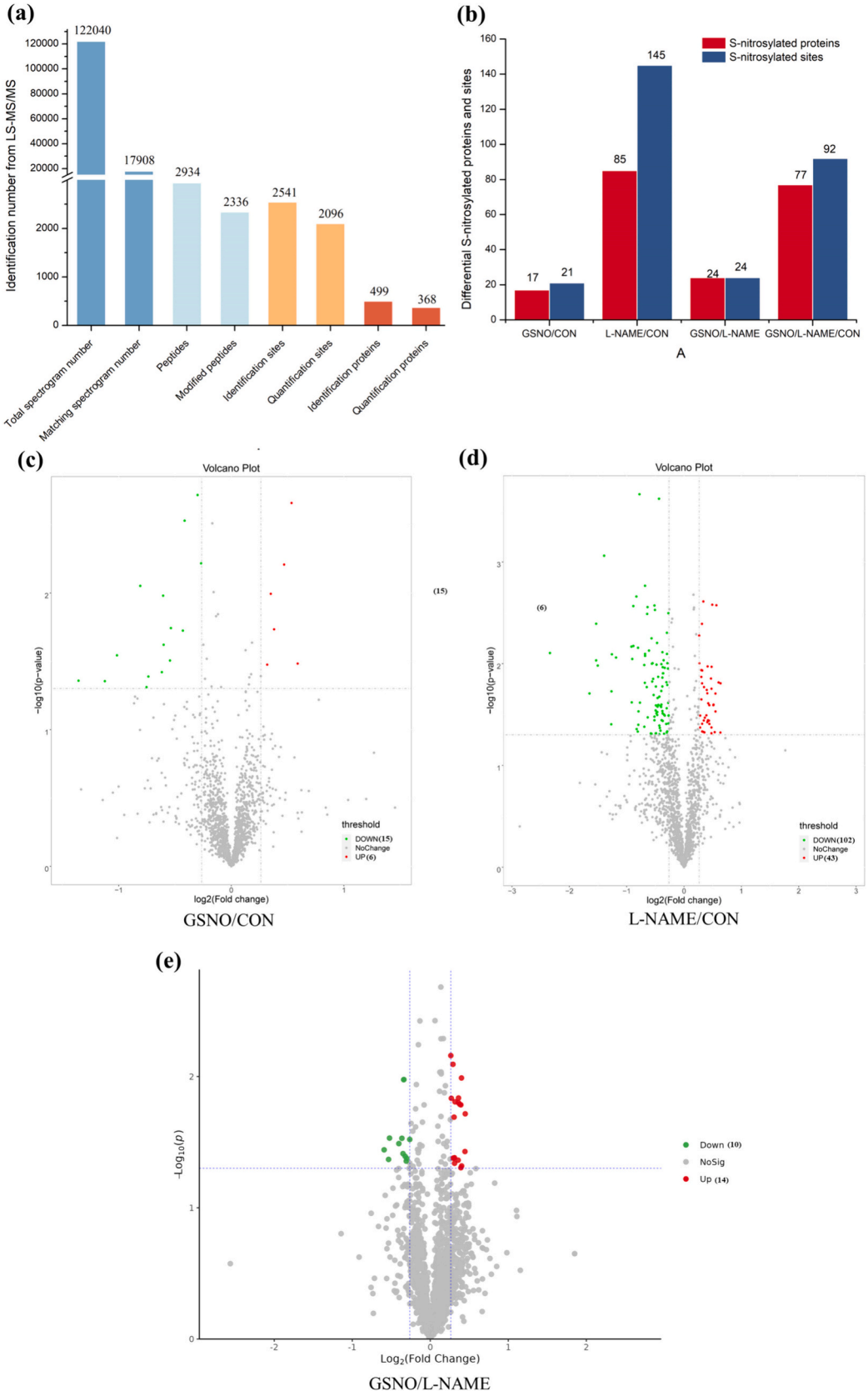

Fig. 3. Quantitative analysis of the S-nitrosoproteome in postmortem beef ($n = 3$). (a) number of total S-nitrosylated proteins and modification sites, (b) Comparison of differentially expressed S-nitrosylated proteins and cysteine sites among different groups, (c-d) Volcano plot of the differential S-nitrosylated sites in GSNO/CON, L-NAME/CON, and GSNO/L-NAME groups. Red dots represent up-regulated S-nitrosylated proteins while blue dots represent down-regulated S-nitrosylated proteins. CON: the control group, GSNO: NO donor group, L-NAME: NOS inhibitor group. (For interpretation of the references to color in this figure legend, the reader is referred to the web version of this article.)

modification in beef SM muscle. This was probably owing to that NOS activity could be retained for a long time in post-mortem beef, as observed in our prior investigation (Hou et al., 2019). With this exciting clue, we further quantitatively compare SNPs among different treatments. Differentially expressed SNPs were screened according to the difference fold >1.2 and $P < 0.05$ and presented in Fig. 3(b). It showed that 85 differential SNPs were detected in the L-NAME/CON group while 17 differential proteins were found in the GSNO/CON group. Besides, analysis of the volcano plot indicated that 43 SNCs belonging to 32 proteins were up-regulated and 102 SNCs on 53 proteins were down-regulated in the L-NAME group (Fig. 3(c-d)). Meanwhile, the GSNO group possessed 6 up-regulated SNCs on 5 proteins and 15 down-regulated SNCs on 12 proteins. As for GSNO/L-NAME group, 10 proteins were down-regulated while 14 proteins were up-regulated (Fig. 3 (e)). To visualize differential SNPs among three groups, clustering analysis was conducted here and the heatmaps of beef samples in triplicate are indicated in Fig. 4 and Supplementary Fig. 3. High variability of SNPs was revealed among the three groups, suggesting different post-mortem metabolic levels in beef SM muscles from the three groups. It is worth mentioning that a subset of identified differential SNPs is suggested to be implicated in early post-mortem conversion of muscle into meat (Table 2), including calcium-releasing-related proteins such as sarcoplasmic reticulum calcium ATPase 1 (SERCA 1) and ryanodine receptor 1 (RyR 1), energy metabolic enzymes such as pyruvate kinase (PK), glyceraldehyde-3-phosphate dehydrogenase (GAPDH), lactate dehydrogenase (LDH), triosephosphate isomerase 1 (TPI), and fructose-bisphosphate aldolase (ALDO), as well as myofibrils and cytoskeletal proteins including actin, nebulin, myosin type II, and plectin. Calpain 3 and cytochrome *b*-c1 complexes that are relevant to muscle fiber development and mitochondrial function were also found to undergo S-nitrosylation modification. The missing of several known S-nitrosylated targets, such as μ-calpain and caspases, might be due to extremely low abundance in beef samples.

SERCA 1 is involved in muscle relaxation by hydrolyzing ATP and re-uptaking cytosolic Ca^{2+} into the sarcoplasmic reticulum. It was demonstrated that S-nitrosylation reversibly inactivated the activity of SERCA1 by targeting a broad spectrum of cysteines towards sites 364, 471 and 670 (Viner et al., 2000). Consistent with this report, we found SERCA1 was S-nitrosylated at four cysteine residues, including Cys 364, Cys 471, Cys 498, and Cys 613, which derived from the peptides of TGTLTTNQMSVC#K, ANAC#NSVIR, KSMSVYC#SPAK, and EVMG-SIQLC#R (Table 2). This was confirmed by Su et al. (2013) that 15 cysteines of SERCA 1 were S-nitrosylated in mouse skeletal muscle through *in vitro* incubation with GSNO, implying the potent regulatory role of S-nitrosylation in SERCA activity. The inactivation of SERCA1 by S-nitrosylation could lead to the elevated calcium concentration in the cytosol (Wang et al., 2019), which triggered the degradation of myofibrillar protein by μ-calpain, thus contributing to meat tenderization (Huff-Lonergan et al., 2010). In addition, RyR1, another crucial mediator of sarcoplasmic calcium homeostasis, was identified to be SNO-modified at Cys2370 (KPEC#FGPALR), supporting the deduction that S-nitrosylation could regulate calcium homeostasis during early post-mortem conversion of muscle into meat and then influence meat quality.

Energy metabolic enzymes are thought to be targets of S-nitrosylation (Lam et al., 2010; Liu et al., 2010). In this study, some of the identified SNPs were recognized as glycolytic enzymes, including PK, GAPDH, LDH, and TPI. The modification sites of these four enzymes were located at Cys 392, Cys 245, Cys 164, and Cys 127, respectively. PK is acknowledged as the rate-limiting factor of glycolysis which underlies the formation mechanism of PSE pork and poultry (Scheffler & Gerrard,

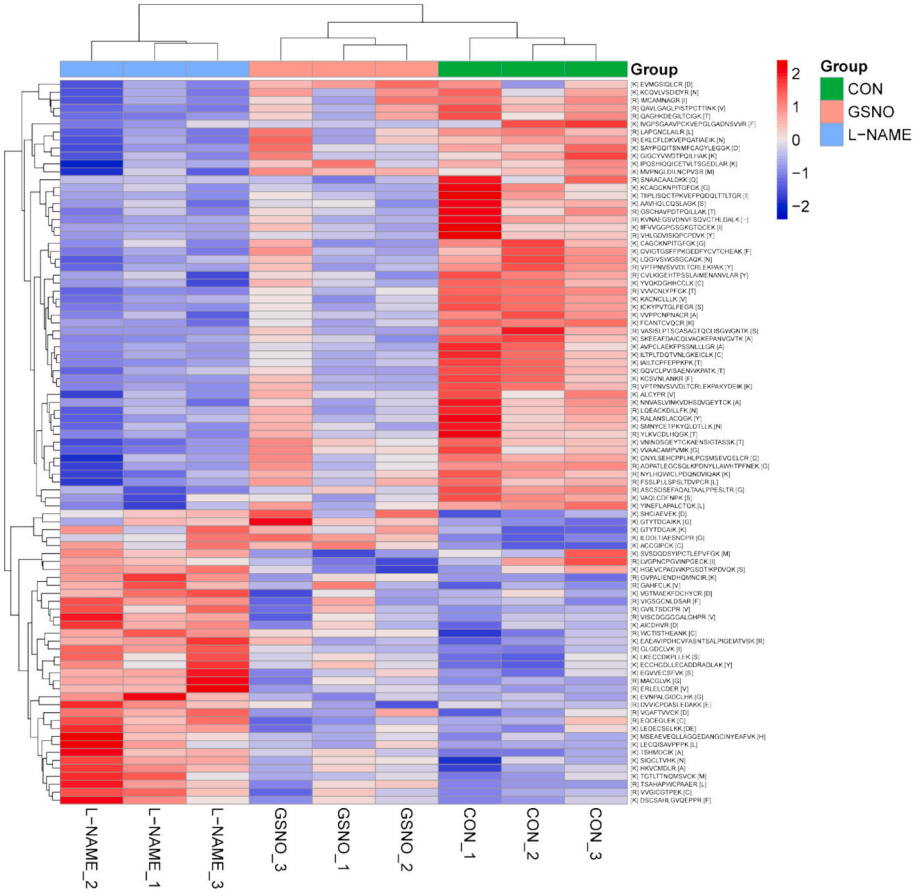

Fig. 4. Heat map of differential SNO-modified proteins in GSNO/L-NAME/CON (n = 3). CON: the control group, GSNO: NO donor group, L-NAME: NOS inhibitor group.

Table 2
Differentially expressed S-nitrosylated proteins and modification sites of beef *semimembranosus* muscles from three cattle among different treatments at 24 h post-mortem.

Protein Name	Protein ID	Gene Name	Annotated Sequence	SNO-Cys sites	P value
Sarcoplasmic/endoplasmic reticulum calcium ATPase 1	Q0VCY0	ATP2A1	[K].TGTLTTNQMSVCK.[M]	Cys364	0.035
			[R].ANACNSVIR.[Q]	Cys471	0.010
			[R].KSMSVYCSPAK.[S]	Cys498	0.021
			[K].EVMGSIQLCR.[D]	Cys613	0.025
Ryanodine receptor 1	A0A3Q1MUQ4	RYR1	[R].KPECFGPALR.[G]	Cys2370	0.039
Pyruvate kinase	Q3ZC87	PKM	[R].AEGSDVANAVLDGADCIMLSGETAK.[G]	Cys392	0.033
Glyceraldehyde-3-phosphate dehydrogenase	P10096	GAPDH	[R].VPTPNVSVVDLTCRLEKPAK.[Y]	Cys245	0.031
Lactate dehydrogenase	B0JYN3	LDHB	[R].VIGSGCNLDSAR.[F]	Cys164	0.004
Triosephosphate isomerase	Q5E956	TPI1	[K].VAHALAEGLGVIACIGEK.[L]	Cys127	0.024
fructose-bisphosphate aldolase	A6QLL8	ALDOA	[R].CVLKIGEHTPSSLAIMENANVLAR.[Y]	Cys150	0.012
			[K].RALANSLACQGK.[Y]	Cys339	0.016
Malate dehydrogenase	Q3T145	MDH1	[K].AICDHVR.[D]	Cys251	0.017
Actin	P68138	ACTA1	[K].EKLCYVALDFENEMATAASSSSLEK.[S]	Cys219	0.031
Nebulin	A0A3Q1MC60	NEB	[K].GKWSETPCFEIATAR.[M]	Cys275	0.048
Myosin-2	F1MRC2	MYH2	[K].LEDECSELKK.[DE]	Cys952	0.036
Plectin	A0A3Q1MQG2	PLEC	[K].VLSGSGSEAAVPSVCFLVPPPNQEALEAVAR.[L]	Cys816	0.005
Calpain-3	F6PWC4	CAPN3	[R].MACGLVK.[G]	Cys329	0.015
Cytochrome b-c1 complex	P00126	UQCRH	[R].ERLELCDER.[V]	Cys53	0.038
Ubiquitin-conjugating enzyme	Q3MHP1	UBE2L3	[K].GQVCLPVISAENWKPATK.[T]	Cys86	0.008

The differential S-nitrosylated proteins and SNO-sites among different treatment groups were screened according to the fold change >1.2 and $P < 0.05$ ($n = 3$). The FDR was for protein identification and the PSM identification was set to 1%.

2007). Wang et al. (2020) further compared the S-nitrosylation extent of PK between PSE and normal pork, elucidating the development of PSE meat from the perspective of the S-nitrosylation impact on glycolysis. In the current study, a higher extent of S-nitrosylated PK was found in the GSNO group ($P < 0.05$), which was in accordance with the results of Zhang et al. (2019) that NO donor treatment improved the S-nitrosylation level of PK whereas decreased its activity. Moreover, the activities of PK, GADPH, LDH, and TPI had a significant correlation with shear force, water-holding capacity, color, and pH value of post-mortem muscles (Ouali et al., 2013; Picard, 2017). Therefore, it is plausible to infer that the modification of glycolytic enzymes by S-nitrosylation could regulate the extent of muscle energy metabolism, which contributes significantly to the formation of meat quality.

Additionally, many myofibrils and cytoskeletal proteins were identified as S-nitrosoproteins, such as actin, nebulin, myosin type II, and plectin (Table 2). This agrees with the reports of Bansbach and Guilford (2016) and Horenberg et al. (2019) that protein S-nitrosylation can influence muscular biological processes through the modification of myofibrillar and cytoskeletal proteins. Plectin is a high-molecular-weight cytoskeletal junction protein, which can connect to actin and microtubule network (Spurny et al., 2007). We previously observed the degradation of plectin during pork aging, which was possibly correlated with skeletal muscle structure changes and water distribution (Tian et al., 2019). Furthermore, it was noted that the expression of plectin was enhanced in abnormal beef *longissimus thoracis* when compared to normal beef (Zhu et al., 2021). These suggest that S-nitrosylation of plectin is a potential pathway for regulating muscle contractile and meat quality. Further, the SNO-modification site of plectin was located at Cys816, which differed from the finding of Zhu et al. (2021) that plectin was SNO-modified at Cys797. The inconsistency may be due to differences in the S-nitrosylation intensity of beef samples. As a synergistic relationship between S-nitrosylated intermediate filament protein and plectin was proposed (Horenberg et al., 2019), it is tempting to infer that S-nitrosylation could influence plectin-intermediate filament networks to regulate meat quality development. Taking together, NO could exert effects on the structure and function changes of crucial muscle proteins through S-nitrosylation modification, thus modulating beef quality.

3.4. Characteristics of differential S-nitrosylated proteins

Protein S-nitrosylation, as a post-translational modification of cysteine thiols into S-NO, commonly occurs at active cysteines to modulate protein function or activity (Thompson et al., 2003). Thus, profiling the characteristics of differential SNP and SNC is essential for figuring out the alteration of structure and function that accounts for the consequent biochemical changes. As illustrated in Fig. 5(a), SNPs were mainly identified as enzymes, indicating a great significance on post-mortem muscle metabolism. This finding was proven by Liu et al. (2019) who concluded that enzyme proteins accounted for a large proportion of SNPs and actively participated in post-mortem pork metabolic processes. In addition to enzymes, cytoskeletal protein, transporter, translational protein, chaperone, protein-binding activity modulator, and extracellular matrix protein were also modified by S-nitrosylation. Diversified differential SNPs facilitate the involvement of S-nitrosylation in various post-mortem biological processes. Then categories of S-nitrosylated enzymes were further investigated. A great variety of S-nitrosylated enzymes was detected in beef SM muscle, including oxidoreductase, transferase, protease, ligase, hydrolase, lyase, isomerase, and kinase (Fig. 5(b)). These are consistent with the demonstration of Hess et al. (2005) that exogenous NO-induced S-nitrosylation could modulate the activities of a broad range of metabolic enzymes, including oxidoreductase, protease, and protein kinases. This implies that S-nitrosylation can expand its functional range in cellular signaling by regulating other post-translational modifications, such as Cys-based redox modification, acetylation, and ubiquitination. Also, previous studies have stated that S-nitrosylation influenced the catalytic activity of proteases, such as μ-calpain as well as caspase-3 to degrade myofibrils and cytoskeletal proteins, which played crucial roles in meat tenderization (Hou et al., 2020; Li et al., 2014; Liu et al., 2016). The regularity of primary sequence motifs from SNC was examined. Three potential motifs were identified including (xMxxxxxxxx_C_xxxxxxxxxx), (xxxxxxxxT_C_xxxxxxxxxx), and (xxxxxxxxxx_C_xxxxRxxxxx). This indicates that the methionine (M), threonine (T), and arginine (R) were flanked at the −9, −1, and + 5 positions of SNO-Cys, respectively (Fig. 5 (c)). Interestingly, methionine is a hydrophobic amino acid and the hydrophobic region of protein can provide micelle-catalyzed sites and facilitate the generation of nitrosylated species, thereby facilitating S-nitrosylation (Stomberski et al., 2019). It was exemplified by RyR1 with the location of SNO-Cys in the hydrophobic region of the calmodulin-binding domain. Substantial hydrophobic amino acids in the flank of SNO-modified cysteine sites were also identified in post-mortem pork (Ma et al., 2023). Furthermore, another critical feature of SNP was proposed by Cheng et al. (2014) that the modified cysteines were surrounded by a large number of base amino acid residues. Similarly, Liu

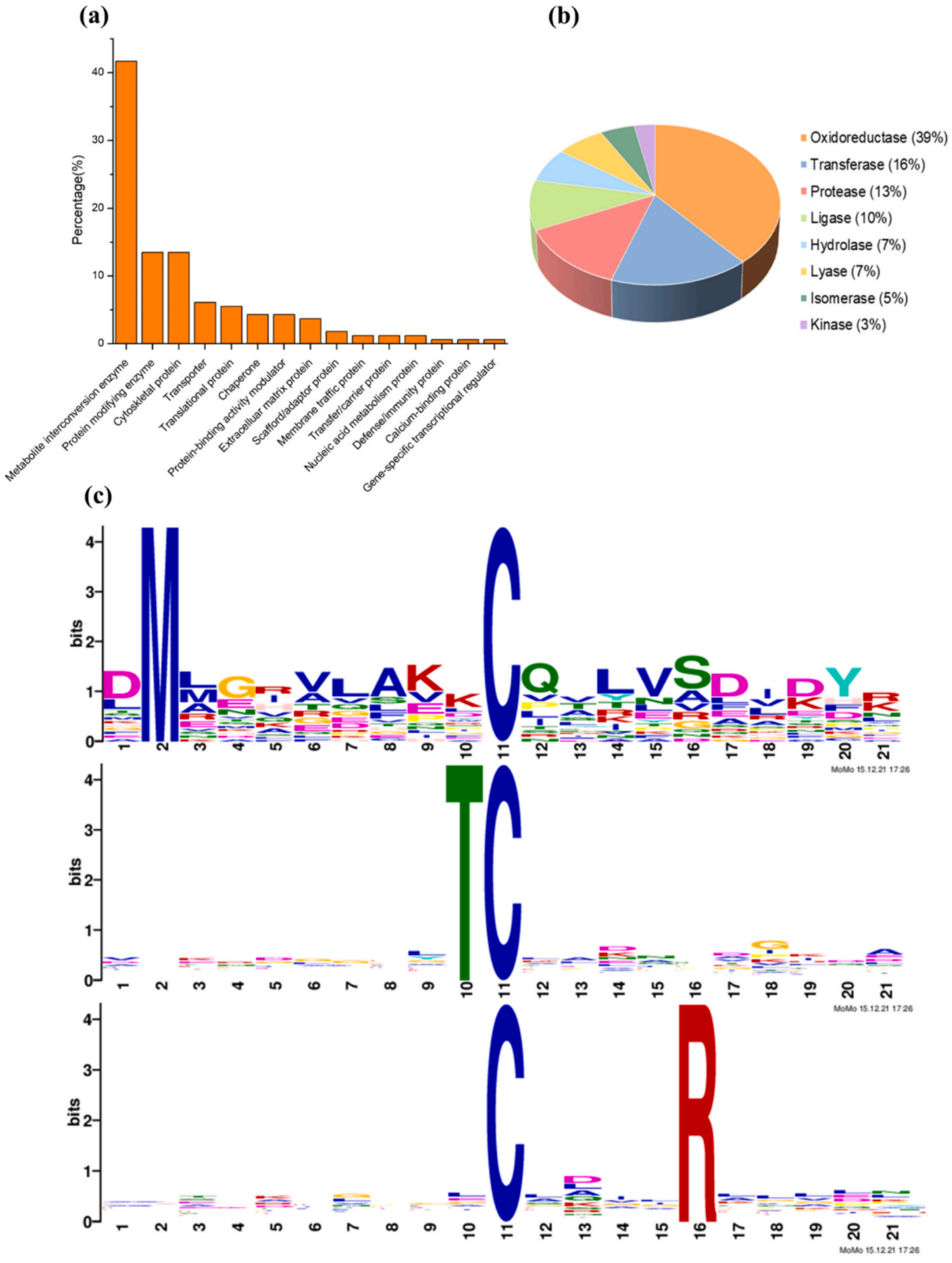

Fig. 5. Characteristics of the identified differential S-nitrosylated proteins and sites. (a) classification of differential S-nitrosylated proteins, (b) distribution of enzymes from SNO-modified proteins, (c) primary sequence motif of differential S-nitrosylated cysteine sites.

et al. (2019) found that all the basic residues (arginine, lysine, and histidine) were flanked with cysteine sites. In the current study, arginine was found in proximity to the observed SNO-Cys, which could promote the deprotonation of thiols and increase the susceptibility of S-nitrosylation. Overall, the identified motifs in this paper were featured by the presence of basic residues and a hydrophobic environment, which facilitates NO to play its cellular signaling roles through the S-nitrosylation pathway.

3.5. GO analysis

GO functional classification of differential SNP was conducted from three aspects including biological process, cellular component, and molecular function to further clarify the roles of SNP in early postmortem conversion of muscle into meat. According to the analysis of biological process, plenty of differential SNPs were implicated in metabolic processes (Fig. 6(a)). Meanwhile, major SNPs were distributed in cytoplasm while few were located in organelle. In terms of molecular function, over half of SNO-target proteins were identified as binding proteins, especially binding with cytoskeletal proteins. Nevertheless, the rest were found to be related to enzymatic activities. The results are similar to the observations of Liu et al. (2019) that SNPs exerted various molecular functions including binding, catalysis, receptor and enzyme-regulator-related activities. In addition, the top 10 GO terms enriched in the GSNO/L-NAME/CON group were investigated. Fig. 6(b) indicated that most SNPs were addressed to terms of catalytic and binding activities and involved in 'carboxylic acid metabolic process', 'oxoacid metabolic process' 'organic acid metabolic process', 'small molecule metabolic process', and 'ATP metabolic process'. Significant enrichments of differential proteins were observed in diverse cellular compartments, including 'cytoplasm', 'mitochondria', and 'sarcolemma'. The subcellular distribution and targeted cysteines of SNP are prerequisites for the occurrence of protein S-nitrosylation (Liu et al., 2018). Thus, the subcellular localization of the identified SNP was examined and illustrated in Fig. 6(c). Among 51 differential SNP, 22 proteins were distributed in the cytoplasm with the highest proportion of 41%, as well as 18 in the membrane (27.45%), 8 in the mitochondrion (15.69%), and 7 in other regions (13.72). This emerging data indicate that that S-nitrosylation occurs in a wide range of cellular components, providing the possibility for S-nitrosylation to participate in various metabolic processes.

3.6. KEGG enrichment pathway analysis

The crucial biochemical pathways that caused differences in beef quality were explored through KEGG enrichment analysis. The results manifested that differential SNPs were engaged in diverse metabolic pathways, such as glycolysis, propanoate metabolism, pyruvate metabolism, glyoxylate metabolism, TCA cycle, fatty acid degradation, cysteine and methionine metabolism, as well as oxidation phosphorylation (Fig. 7). Thereinto, glycolysis was found to be the most significantly enriched pathway. To check into the differential SNPs in multiple metabolic processes, the pathways of glycolysis, pyruvate metabolism, and TCA cycle were further analyzed. Admittedly, glycolysis is the primary energy metabolic process in post-mortem muscle, which is critical to the development of meat quality (Ren et al., 2024). In glycolysis, five glycolytic enzymes were modified by S-nitrosylation in beef SM muscle, including PK, GAPDH, LDH, ALDO, and TPI. It was found that the expression of S-nitrosylated PK was up-regulated in the GSNO/CON group while S-nitrosylated GAPDH was down-regulated (Supplementary Fig. 4(a)). Meanwhile, one up-regulated SNP (LDH) and three down-regulated SNPs (GAPDH, ALDO, and TPI) were observed in the L-

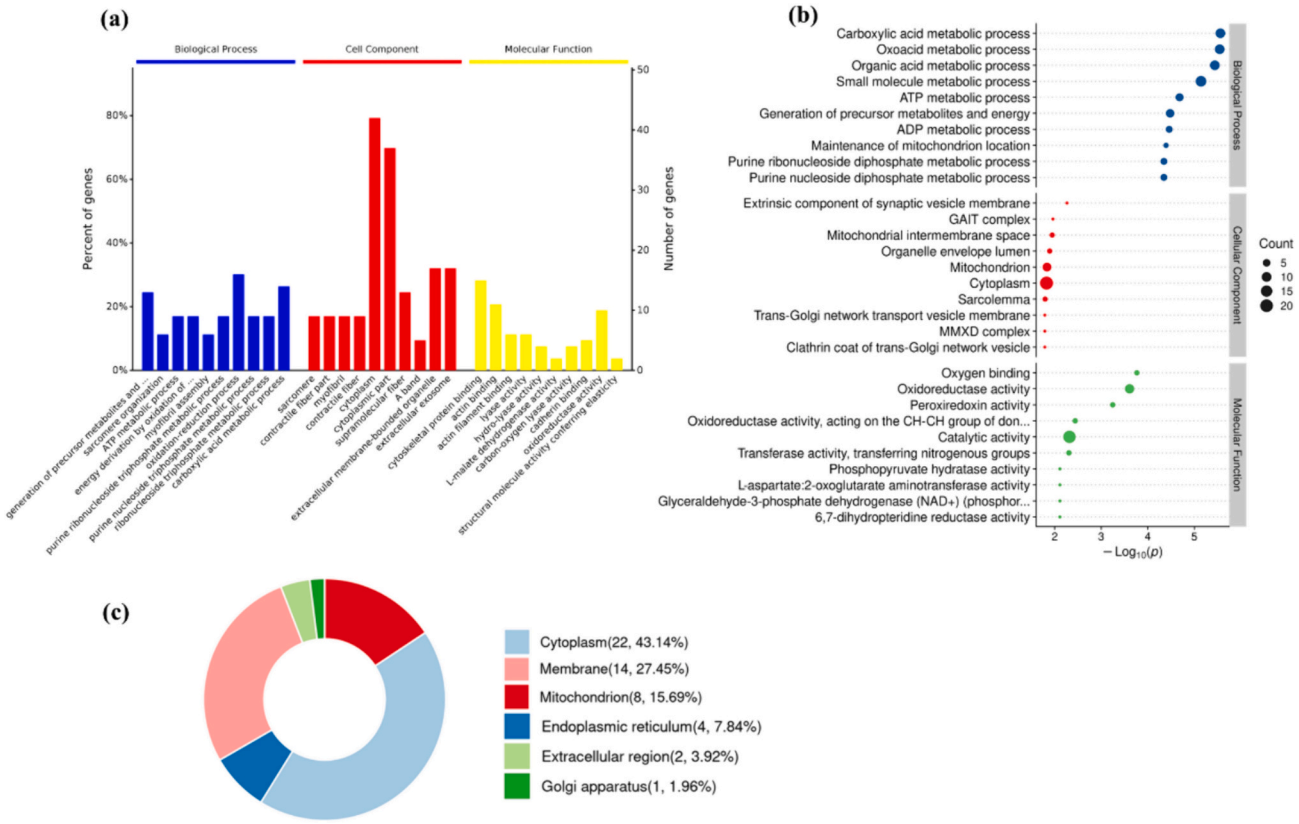

Fig. 6. Gene ontology analysis of differential S-nitrosylated proteins among different groups. (a) GO functional classifications including biological process, cellular component, and molecular function, (b) top 10 GO terms enriched in GSNO/L-NAME/CON group, (c) subcellular localization of S-nitrosylated proteins. CON: the control group, GSNO: NO donor group, L-NAME: NOS inhibitor group.

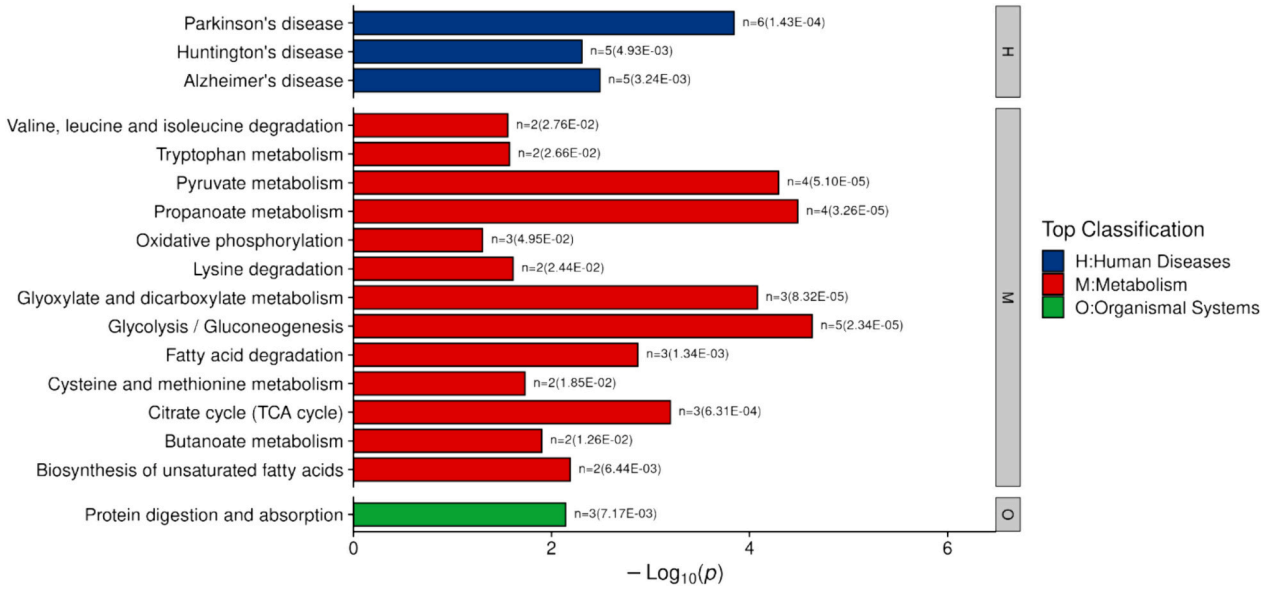

Fig. 7. KEGG enrichment analysis of differential S-nitrosylated proteins in postmortem beef among different groups.

NAME/CON group (Supplementary Fig. 4 (b)). PK is in charge of catalyzing the conversion of phosphoenolpyruvate to pyruvate in the final step of glycolysis. In a prior study, higher pyruvate content was observed in low-pH beef accompanied by increased tenderness, indicating that PK activity was involved in prompting beef tenderization (Zhao et al., 2022). Besides, higher activity of PK was detected in pale, soft, and exudative pork, which could be putatively concerned with the lower S-nitrosylation extent of PK (Wang et al., 2020), suggesting that S-nitrosylation could partly regulate post-mortem glycolysis by modulating PK activity. This finding was evidenced by Jaffrey et al. (2001) who demonstrated that the reactive cysteine thiols of PK were easily modified by S-nitrosylation when exposed to NO. As noted above, it is reasonable to speculate that GSNO treatment elevated the S-nitrosylation level of PK, which could inactivate PK activity, thus resulting in higher pH and decreased tenderness of beef SM muscle. GAPDH is also recognized as the crucial enzyme of the glycolysis process. S-nitrosylation, as a mediator of GAPDH, could prevent GAPDH from oxidant inactivation to modulate glycolysis (Zhang et al., 2019). Also, S-nitrosylated GAPDH can interact with ubiquitin ligase after transduction into the nucleus, which could activate ubiquitinase activity and lead to the degradation of nuclear target proteins by nuclear translocation and protein ubiquitination, thus initiating apoptosis (Benhar & Stamler, 2005). Besides, the catalytic activity of ALDO was restrained after NO donor treatment *in vitro* which was conversely proportional to the S-nitrosylation of ALDO (Yan et al., 2011). Intriguingly, all SNO-target glycolytic enzymes including GADPH, LDH, PK, ALDO, and TPI were related to meat quality (Ouali et al., 2013; Picard, 2017). As such, accumulating evidences point towards crucial roles of S-nitrosylation in glycolysis, which underlies the mechanism of S-nitrosylation in regulating beef quality. In pyruvate metabolism, three SNPs were identified including LDH, MDH, and acetyl-CoA acetyltransferase (ACAT), with LDH and MDH expression being up-regulated while ACAT expression being down-regulated in the L-NAME group. MDH is a homodimeric enzyme that catalyzes the transformation of malate into oxaloacetate (Sew et al., 2016). Interestingly, MDH was also enriched in the TCA cycle and up-regulated in the L-NAME/CON group. From above, it suggests that carbohydrate metabolism especially glycolysis was the most significant pathway that SNPs were involved in the development of beef quality. In addition to carbohydrate metabolism, S-nitrosylation could play potential roles in regulating oxidative stress and mitochondrial dysfunction through modifying antioxidant enzymes and cytochrome *c*-related enzymes in post-mortem muscles. The S-nitrosylation modification of specific proteins related to oxidative stress and mitochondrial homeostasis should be further studied.

3.7. PPI network analysis

In the current study, a String Network was generated (Fig. 8) based on fold changes of protein expression, PPIs, and KEGG pathway and biological process enrichments. In total, 36 SNPs were identified as circular nodes connected with each other, representing a comprehensive PPI network of beef SM muscle. The results showed that MDH1, MDH2, LDHA, GAPDH, TPI1, ALDOA, and GOT2 displayed a high degree. Besides, six clusters of highly enriched interaction were detected, including pyruvate metabolism, cysteine and methionine metabolism, glycolysis, biosynthesis of amino acid, glyoxylate and dicarboxylate metabolism, as well as oxidative phosphorylation, which is in agreement with the analysis of KEGG pathways (Fig. 7). Similar results are reported by Ma et al. (2023) that glycolysis/gluconeogenesis, biosynthesis of amino acid, and oxidative phosphorylation were identified as the enrichment pathways involved in post-mortem pork metabolism. After slaughter, oxygen in muscle cells steadily declined during 2 h post-mortem rather than instantly depleted (Matarneh et al., 2021). This clarifies that mitochondrial oxidative phosphorylation could occur in the early stage of post-mortem muscle, thus producing ATP for muscle cells (Ma et al., 2023). The glycolytic pathway was activated in muscle cells under oxygen depletion (Zhang et al., 2019). Meanwhile, the consumption of pyruvate was accelerated by protein S-nitrosylation (Lu et al., 2022). The pivotal roles of S-nitrosylation in the regulation of glycolysis and pyruvate metabolism were validated by Qiu et al. (2019). As noted above, NO-induced S-nitrosylation potentially regulate metabolic processes and then participate in the development of meat quality.

4. Conclusion

In summary, employing NO donors or NOS inhibitors to manipulate S-nitrosation levels of beef SM muscles was proven to exert significant impacts on beef quality. To further explore the mechanism of S-nitrosylation on beef quality, the first comprehensive S-nitrosylation profiling of SM muscles was performed by iodoTMT-based S-nitrosoproteomics. It was found that a great variety of muscle proteins including energy metabolic enzymes, calcium-releasing mediators, myofibrillar and cytoskeleton proteins were identified as S-nitrosylated proteins and differentially expressed among treatments. Furthermore,

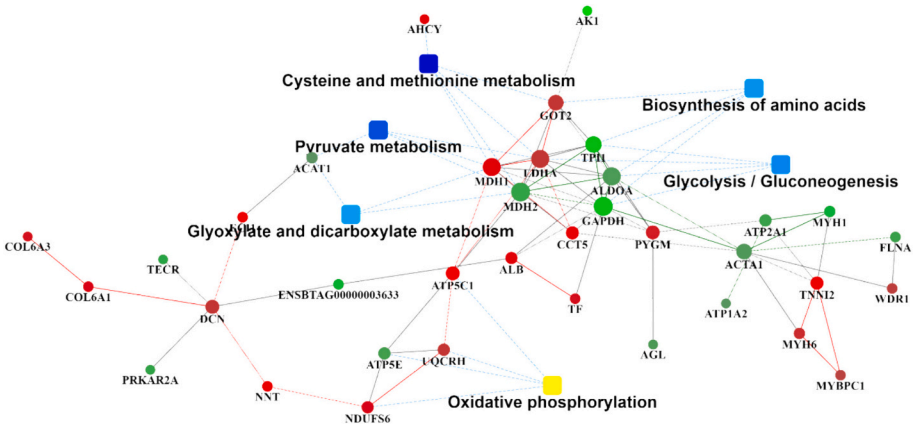

Fig. 8. String network of differential S-nitrosylated proteins in beef *semimembranosus* muscles among different groups. Circular nodes represent proteins, while rectangles represent KEGG pathways or GO biological processes. The color of the rectangle ranges from yellow to blue, with the bluer indicating more significant functional enrichment. The circular nodes change from green to red, with red indicating upregulated proteins and green indicating downregulated proteins. (For interpretation of the references to color in this figure legend, the reader is referred to the web version of this article.)

GO and KEGG analysis revealed that the identified differential proteins were widely distributed in subcellular compartments, in particular cytoplasm, which provides a possibility that S-nitrosylated proteins could participate in various post-mortem metabolic pathways. Notably, glycolysis was found to be the most significantly enriched metabolic pathway. Collectively, these observations support that the modification of crucial muscle proteins by S-nitrosylation could be involved in the regulation of post-mortem metabolic pathways, thereby affecting the development of beef quality.

CRediT authorship contribution statement

Qin Hou: Writing – review & editing, Writing – original draft, Software, Methodology, Formal analysis, Data curation. **Tianyi Gao:** Methodology, Investigation, Formal analysis, Data curation. **Rui Liu:** Validation, Methodology. **Chao Ma:** Validation, Methodology. **Wangang Zhang:** Supervision, Resources.

Declaration of competing interest

None.

Data availability

Data will be made available on request.

Acknowledgments

This study was supported by the funding of National Natural Science Foundation of China (32301970; 31871827), and Yangzhou University (137012844). The technical support of Shanghai Bioprofile Biotechnology Co., Ltd. is acknowledged.

Appendix A. Supplementary data

Supplementary data to this article can be found online at https://doi.org/10.1016/j.meatsci.2024.109580.

References

Alderton, W. K., Cooper, C. E., & Knowles, R. G. (2001). Nitric oxide synthases: Structure, function and inhibition. *Biochemical Journal, 357*(3), 593–615.
Bansbach, H. M., & Guilford, W. H. (2016). Actin nitrosylation and its effect on myosin driven motility. *AIMS Molecular Science, 3*(3), 426–438.
Benhar, M., & Stamler, J. S. (2005). A central role for S-nitrosylation in apoptosis. *Nature Cell Biology, 7*(7), 645–646.
Biffin, T. E., Smith, M. A., Bush, R. D., Morris, S., & Hopkins, D. L. (2020). The effect of whole carcase medium voltage electrical stimulation, tenderstretching and longissimus infusion with actinidin on alpaca meat quality. *Meat Science, 164*, Article 108107.
Brannan, R. G., & Decker, E. A. (2002). Nitric oxide synthase activity in muscle foods. *Meat Science, 62*(2), 229–235.
Cheng, S., Shi, T., Wang, X. L., Liang, J., Wu, H., Xie, L., & Zhao, Y. L. (2014). Features of S-nitrosylation based on statistical analysis and molecular dynamics simulation: Cysteine acidity, surrounding basicity, steric hindrance and local flexibility. *Molecular BioSystems, 10*(10), 2597–2606.
Cottrell, J. J., McDonagh, M. B., Dunshea, F. R., & Warner, R. D. (2008). Inhibition of nitric oxide release pre-slaughter increases post-mortem glycolysis and improves tenderness in ovine muscles. *Meat Science, 80*(2), 511–521.
Figueired, C., Dulce, R. A., Foster, M. W., Liang, J., Yamashita, A. M., Lima-Rosa, F. L., & Nogueira, L. (2015). S-nitrosylation of sarcomeric proteins depresses myofilament Ca^{2+} sensitivity in intact cardiomyocytes. *Antioxidants & Redox Signaling, 23*(13), 1017–1034.
Forrester, M. T., Thompson, J. W., Foster, M. W., Nogueira, L., Moseley, M. A., & Stamler, J. S. (2009). Proteomic analysis of S-nitrosylation and denitrosylation by resin-assisted capture. *Nature Biotechnology, 27*(6), 557–559.
Hess, D. T., Matsumoto, A., Kim, S. O., Marshall, H. E., & Stamler, J. S. (2005). Protein S-nitrosylation: Purview and parameters. *Nature Reviews Molecular Cell Biology, 6*(2), 150–166.
Horenberg, A. L., Houghton, A. M., Pandey, S., Seshadri, V., & Guilford, W. H. (2019). S-nitrosylation of cytoskeletal proteins. *s, 76*(3), 243–253.
Hou, Q., Liu, R., Zhang, W. G., & Zhou, G. H. (2019). Nitric oxide synthase in beef semimembranosus muscle during post-mortem aging. *Food Chemistry, 288*, 187–192.
Hou, Q., Zhang, C. Y., Zhang, W. G., Liu, R., Tang, H. Q., & Zhou, G. H. (2020). Role of protein S-nitrosylation in regulating beef tenderness. *Food Chemistry, 306*, Article 125616.
Hou, Q., Zhu, Q. N., Lu, W. W., & Zhang, W. G. (2022). Protein S-nitrosylation regulates post-mortem beef apoptosis through the intrinsic mitochondrial pathway. *Journal of Agricultural and Food Chemistry, 70*(4), 1252–1260.
Huff-Lonergan, E. H., Zhang, W., & Lonergan, S. M. (2010). Biochemistry of post-mortem muscle-lessons on mechanisms of meat tenderization. *Meat Science, 86*(1), 184–195.
Jaffrey, S. R., Erdjument, B. H., Ferris, C. D., Tempst, P., & Snyder, S. H. (2001). Protein S-nitrosylation: A physiological signal for neuronal nitric oxide. *Nature Cell Biology, 3*, 193–197.
Lam, Y. W., Yuan, Y., Isaac, J., Babu, C. S., Meller, J., & Ho, S. M. (2010). Comprehensive identification and modified-site mapping of S-nitrosylated targets in prostate epithelial cells. *PLoS One, 5*(2), 9075.
Li, Y. P., Liu, R., Zhang, W. G., Fu, Q. Q., Liu, N., & Zhou, G. H. (2014). Effect of nitric oxide on μ-calpain activation, protein proteolysis, and protein oxidation of pork during post-mortem aging. *Journal of Agricultural and Food Chemistry, 62*(25), 5972–5977.
Liu, H., Ma, J. R., Pan, T., Raheel, S., Wang, Z. Y., & Zhang, D. Q. (2021). Effects of roasting by charcoal, electric, microwave and superheated steam methods on (non) volatile compounds in oyster cuts of roasted lamb. *Meat Science, 172*, Article 108324.
Liu, M., Hou, J., Huang, L., Huang, X., Heibeck, T. H., Zhao, R., … Ding, S. J. (2010). Site-specific proteomics approach for study protein S-nitrosylation. *Analytical Chemistry, 82*(17), 7160–7168.
Liu, R., Li, Y. P., Wang, M. Q., Zhou, G. H., & Zhang, W. G. (2016). Effect of protein S-nitrosylation on autolysis and catalytic ability of μ-calpain. *Food Chemistry, 213*, 470–477.
Liu, R., Warner, R. D., Zhou, G. H., & Zhang, W. G. (2018). Contribution of nitric oxide and protein S-nitrosylation to variation in fresh meat quality. *Meat Science, 2018* (144), 135–148.
Liu, R., Zhang, C. Y., Xing, L. J., Zhang, L. L., Zhou, G. H., & Zhang, W. G. (2019). A bioinformatics study on characteristics, metabolic pathways, and cellular functions

of the identified S-nitrosylated proteins in post-mortem pork muscle. *Food Chemistry, 274*, 407–414.
Lu, W. W., Hou, Q., & Zhang, W. G. (2022). Protein S-nitrosylation regulates the energy metabolism of early post-mortem pork using the *in vitro* model. *Food Materials Research, 2*, 1–8.
Ma, C., Zhang, W. G., Zhang, J., & Du, T. Y. (2023). Modification-specific proteomic analysis reveals cysteine S-nitrosylation mediated the effect of preslaughter transport stress on pork quality development. *Journal of Agricultural and Food Chemistry, 71*, 20260–20273.
Matarneh, S. K., Yen, C. N., Bodmer, J., El-Kadi, S. W., & Gerrard, D. E. (2021). Mitochondria influence glycolytic and tricarboxylic acid cycle metabolism under post-mortem simulating conditions. *Meat Science, 172*, Article 107316.
Miller, M., & Megson, I. (2007). Recent developments in nitric oxide donor drugs. *British Journal of Pharmacology, 151*(3), 305–321.
Moller, J. K. S., & Skibsted, L. H. (2002). Nitric oxide and myoglobins. *Chemical Reviews, 102*(4), 1167–1178.
Ouali, A., Gagaoua, M., Boudida, Y., Becila, S., Boudjellal, A., Herrera-Mendez, C. H., & Sentandreu, M. A. (2013). Biomarkers of meat tenderness: Present knowledge and perspectives in regards to our current understanding of the mechanisms involved. *Meat Science, 95*(4), 854–870.
Picard, B. (2017). Proteomic investigations of beef tenderness. In M. L. Colgrave (Ed.), *Proteomics in food science* (pp. 177–197). Academic Press.
Qiu, C., Sun, J. H., Wang, Y., Sun, L. T., Xie, H., … Ding, Z. T. (2019). First nitrosoproteomic profling deciphers the cysteine S-nitrosylation involved in multiple metabolic pathways of tea leaves. *Scientific Reports, 9*(1), 17525.
Qu, Z., Meng, F., Bomgarden, R. D., Viner, R. I., Li, J., Rogers, J. C., & Lubahn, D. B. (2014). Proteomic quantification and site-mapping of S-nitrosylated proteins using isobaric iodoTMT reagents. *Journal of Proteome Research, 13*(7), 3200–3211.
Ren, C., Bai, Y. Q., Schroyen, M., Hou, C. L., Li, X., … Zhang, D. Q. (2024). Phosphofructokinase mainly affects glycolysis and influences meat quality in post-mortem meat. *Food Bioscience, 58*, Article 103776.
Scheffler, T., & Gerrard, D. (2007). Mechanisms controlling pork quality development: The biochemistry controlling post-mortem energy metabolism. *Meat Science, 77*(1), 7–16.
Sew, Y. S., Ströher, E., Fenske, R., & Millar, A. H. (2016). Loss of mitochondrial malate dehydrogenase activity alters seed metabolism impairing seed maturation and post-germination growth in arabidopsis. *Plant Physiology, 171*(2), 849–863.
Spurny, R., Abdoulrahman, K., Janda, L., Ruonzler, D., Koohler, G., Castanon, M. J., & Wiche, G. (2007). Oxidation and nitrosylation of cysteines proximal to the intermediate filament (IF)-binding site of plectin: Effects on structure and vimentin binding and involvement in IF collapse. *Journal of Biological Chemistry, 282*(11), 8175–8187.
Stamler, J. S., Sun, Q. A., & Hess, D. T. (2008). A SNO storm in skeletal muscle. *Cell, 133*(1), 33–35.
Stomberski, C. T., Hess, D. T., & Stamler, J. S. (2019). Protein S-nitrosylation: Determinants of specificity and enzymatic regulation of S-nitrosothiol-based signaling. *Antioxidants & Redox Signaling, 30*(10), 1331–1351.
Su, D., Shukla, A. K., Chen, B., Kim, J. S., Nakayasu, E., Qu, Y., … Qian, W. J. (2013). Quantitative site-specific reactivity profiling of S-nitrosylation in mouse skeletal muscle using cysteinyl peptide enrichment coupled with mass spectrometry. *Free Radical Biology and Medicine, 57*, 68–78.
Thompson, A., Schäfer, J., Kuhn, K., Kienle, S., Schwarz, J., … Hamon, C. (2003). Tandem mass tags: A novel quantification strategy for comparative analysis of complex protein mixtures by MS/MS. *Analytical Chemistry, 75*(8), 1895–1904.
Tian, X. N., Wang, Y. Y., Fan, X. Q., Shi, Y. W., Zhang, W. G., … Zhou, G. H. (2019). Expression of pork plectin during post-mortem aging. *Journal of Agricultural and Food Chemistry, 67*, 11718–11727.
Viner, R. I., Williams, T. D., & Schöneich, C. (2000). Nitric oxide-dependent modification of the sarcoplasmic reticulum ca-ATPase: Localization of cysteine target sites. *Free Radical Biology & Medicine, 29*(6), 489–496.
Wang, P. G., Xian, M., Tang, X. P., Wu, X. J., Wen, Z., Cai, T. W., & Janczuk, A. J. (2002). Nitric oxide donors: Chemical activities and biological applications. *Chemical Reviews, 102*(4), 1091–1134.
Wang, Y. Y., Liu, R., Hou, Q., Tian, X. N., Fan, X. Q., … Zhou, G. H. (2020). Comparison of activity, expression and S-nitrosylation of glycolytic enzymes between pale, soft and exudative and red, firm and non-exudative pork during post-mortem aging. *Food Chemistry, 314*, Article 126203.
Wang, Y. Y., Liu, R., Tian, X. N., Fan, X. Q., Shi, Y. W., Zhang, W. G., … Zhou, G. H. (2019). Comparison of activity, expression, and S-nitrosylation of calcium transfer proteins between pale, soft, and exudative and red, firm, and non-exudative pork during post-mortem aging. *Journal of Agricultural and Food Chemistry, 67*, 3242–3248.
Yan, J., Shi, Q., Chen, Z., Zhuang, R., Chen, H., Zhu, D., & Lou, Y. (2011). Skeletal muscle aldolase an overexpression in endotoxemic rats and inhibited by GSNO via potential role for S-nitrosylation in vitro. *Journal of Surgical Research, 170*(1), 57–63.
Zhang, C. Y., Liu, R., Wang, A. R., Kang, D. C., Zhou, G. H., & Zhang, W. G. (2018). Regulation of calpain-1 activity and protein proteolysis by protein S-nitrosylation in post-mortem beef. *Meat Science, 141*, 44–49.
Zhang, L. L., Liu, R., Cheng, Y., Xing, L., Zhou, G. H., & Zhang, W. G. (2019). Effects of protein S-nitrosylation on the glycogen metabolism in post-mortem pork. *Food Chemistry, 272*, 613–618.
Zhang, W. G., Marwan, A. H., Samaraweera, H., Lee, E. J., & Ahn, D. U. (2013). Breast meat quality of broiler chickens can be affected by managing the level of nitric oxide. *Poultry Science, 92*(11), 3044–3049.
Zhao, Y., Kong, X., Yang, X., Zhu, L., Liang, R., Luo, X., … Zhang, Y. (2022). Effect of energy metabolism and proteolysis on the toughness of intermediate ultimate pH beef. *Meat Science, 188*, Article 108798.
Zhu, Q. N., Xing, L. J., Hou, Q., Liu, R., & Zhang, W. G. (2021). Proteomics identification of differential S-nitrosylated proteins between the beef with intermediate and high ultimate pH using isobaric iodoTMT switch assay. *Meat Science, 172*, 10832.